Thermodynamic properties of $Yb_2Ti_2O_7$ pyrochlore as a function of temperature and magnetic field: Validation of a quantum spin ice exchange Hamiltonian

N. R. Hayre,[1] K. A. Ross,[2,3,4] R. Applegate,[1] T. Lin,[5] R. R. P. Singh,[1] B. D. Gaulin,[2,6,7] and M. J. P. Gingras[5,7,8]

[1]*Physics Department, University of California at Davis, Davis, California 95616, USA*

[2]*Department of Physics and Astronomy, McMaster University, Hamilton, Ontario, Canada L8S 4M1*

[3]*Institute for Quantum Matter and Department of Physics and Astronomy, Johns Hopkins University, Baltimore, Maryland 21218, USA*

[4]*NIST Center for Neutron Research, National Institute of Standards and Technology, Gaithersburg, Maryland 20899, USA*

[5]*Department of Physics and Astronomy, University of Waterloo, Waterloo, Ontario, Canada N2L 3G1*

[6]*Brockhouse Institute for Materials Research, McMaster University, Hamilton, Ontario, Canada L8S 4M1*

[7]*Canadian Institute for Advanced Research, 180 Dundas St. W., Toronto, Ontario, Canada M5G 1Z8*

[8]*Perimeter Institute for Theoretical Physics, 31 Caroline North, Waterloo, Ontario, Canada N2L 2Y5*

(Received 22 November 2012; revised manuscript received 28 March 2013; published 20 May 2013)

The thermodynamic properties of the pyrochlore $Yb_2Ti_2O_7$ material are calculated using the numerical linked-cluster calculation method for an effective anisotropic-exchange spin-$\frac{1}{2}$ Hamiltonian with parameters recently determined by fitting the neutron scattering spin-wave data obtained at high magnetic field. Magnetization $M(T,h)$ as a function of temperature T and for different magnetic fields h applied along the three high-symmetry directions [100], [110], and [111] are compared with experimental measurements on the material for temperature $T > 1.8$ K. The excellent agreement between experimentally measured and calculated $M(T,h)$ over the entire temperature and magnetic field ranges considered provides strong quantitative validation of the effective Hamiltonian. It also confirms that fitting the high-field neutron spin-wave spectra in the polarized paramagnetic state is an excellent method for determining the microscopic exchange constants of rare-earth insulating magnets that are described by an effective spin-$\frac{1}{2}$ Hamiltonian. Finally, we present results which demonstrate that a recent analysis of the polarized neutron scattering intensity of $Yb_2Ti_2O_7$ using a random phase approximation method [Chang *et al.*, Nat. Commun. **3**, 992 (2012)] does not provide a good description of $M(T,h)$ for $T \lesssim 10$ K, that is, in the entire temperature regime where magnetic correlations become non-negligible. With the compelling evidence that we now have at hand an accurate microscopic Hamiltonian for $Yb_2Ti_2O_7$, our work exposes a paradox: why does this material fail to develop long-range ferromagnetic order?

DOI: 10.1103/PhysRevB.87.184423 PACS number(s): 75.10.Jm, 75.40.Cx, 75.47.Lx, 75.30.Et

I. INTRODUCTION

A. Magnetic rare-earth pyrochlore oxides and effective spin-$\frac{1}{2}$ quantum dynamics

Quantum spin liquids are magnetic systems in which large quantum mechanical zero-point spin fluctuations prevent the development of long-range order down to absolute zero temperature. The search for real materials that display this phenomenology in two and three dimensions is a very active research topic in the field of condensed matter physics.[1] The interest in spin liquids stems from the expectation that they may host nontrivial quantum entanglement, topological order, as well as emergent fractionalized and deconfined low-energy excitations. Spin liquids have also been conjectured as progenitors of unconventional superconductivity at "high temperature." Highly frustrated magnets are particularly apt at exhibiting large quantum spin fluctuations. These magnets are realized in systems which consist of localized magnetic moments (spins) that reside on two- and three-dimensional lattices of corner-sharing triangles or tetrahedra and which interact with effective antiferromagnetic nearest-neighbor coupling.[2] Such highly frustrated magnets display an exponentially large number of classical ground states.[4] This allows for quantum mechanical effects to be tremendously magnified compared to magnetic systems with conventional long-range magnetic order.[1]

The pyrochlore oxides, with chemical formula $RE_2M_2O_7$,[5] count a multitude of magnetic members. In $RE_2M_2O_7$, RE is a magnetic trivalent (lanthanide, $4f$) rare-earth ion (Gd^{3+}, Tb^{3+}, Dy^{3+}, Ho^{3+}, Er^{3+}, Yb^{3+}) or a nonmagnetic ion (Y^{3+}, Lu^{3+}), while M is tetravalent, typically a transition-metal ion, which can be either magnetic (Mo^{4+}, Mn^{4+}) or not (Ti^{4+}, Sn^{4+}, Zr^{4+}, Ge^{4+}). Of relevance to the above discussion is the fact that the RE and M ions reside on two distinct and interpenetrating three-dimensional lattices of corner-sharing tetrahedra. As a result, high geometric magnetic frustration ensues whenever the RE-RE or M-M interaction is effectively antiferromagnetic.[2] Among the $RE_2M_2O_7$ family, the magnetic rare-earth oxides, in which the RE is magnetic and M is not, have been rather extensively studied.[5] These have revealed a number of fascinating phenomena such as long-range order induced by order-by-disorder,[6,7] multiple-k long-range-ordered phase,[8] spin liquid behavior,[9] and spin ice physics,[10–12] the latter having attracted much interest.[1,3,5,13,14] The spin ice state displays a residual low-temperature magnetic entropy close to that found for common water ice,[12,15,16] hence the name spin ice. Most recently, a renewed flurry of theoretical and experimental efforts have been directed at the study of spin ices for they have been argued to display an emergent Coulomb phase[17] accompanied at low energies by deconfined fractionalized magnetic charge excitations, or "monopoles."[14,17,18]

Notwithstanding the rich physics that $RE_2M_2O_7$ materials display,[5] they had, until very recently,[19–22] not attracted that much interest from the community of theorists and experimentalists searching for quantum spin liquids.[1] Quantum

fluctuations are expected to be, relatively speaking, more significant the smaller the spin quantum number $\boldsymbol{S}$. On the other hand, because of the intrinsic large spin-orbit coupling at play in the lanthanide $4f$ series, the total angular momentum $\boldsymbol{J} = \boldsymbol{L} + \boldsymbol{S}$, and not $\boldsymbol{S}$, is a good quantum number with J being typically large across the whole lanthanide series (e.g., $J = 8$ and $J = S = \frac{7}{2}$ for free Ho^{3+} and Gd^{3+} ions, respectively). This situation would thus seem unpromising to those seeking magnetic materials with potentially large quantum mechanical spin fluctuations and exotic quantum states of matter. However, such a perspective is perhaps too pessimistic as we now discuss.

In insulating magnetic compounds with $4f$ elements, the various interion interactions $H_{\rm int}$ (exchange, superexchange, virtual phonon exchange, and magnetostatic dipole-dipole coupling) are typically weak compared to the single-ion crystal-field interactions defined by the crystal-field Hamiltonian $H_{\rm cf}$. As a first approximation, one thus often proceeds by determining the energy level spectrum of $H_{\rm cf}$ for a fixed J manifold.[3] The point group symmetry of the crystal dictates the allowed symmetry properties of $H_{\rm cf}$. These symmetries determine, in return, the spectral decomposition of the crystal-field states that derive from the original $2J + 1$ degenerate $^{2S+1}L_J$ electronic ground state of the otherwise free RE^{3+} ion. In the simplest case, the resulting crystal-field ground state is a magnetic doublet with wave functions $|\psi^+\rangle$ and $|\psi^-\rangle$ that have $|\psi^\pm\rangle = \sum_{m_J} C^\pm_{m_J} |J,m_J\rangle$ for spectral decomposition. The $|\psi^\pm\rangle$ states contain *all* the $|J,m_J\rangle$ spectral components that transform similarly according to the point group symmetry operations. Consequently, there may or not be nonzero $\langle\psi^\pm|H_{\rm int}|\psi^\mp\rangle$ matrix elements. This depends on the specific nature of the interion couplings $H_{\rm int}(J_i^u)$, a function of the components J_i^u $(u = x,y,z)$ of the angular momentum $\boldsymbol{J}_i$ of ion i,[23] as well as the specific ion-dependent spectral decomposition of $|\psi^\pm\rangle$. It is the nonzero $\langle\psi^\pm|H_{\rm int}|\psi^\mp\rangle$ matrix elements[24] which determine whether significant quantum dynamics exist within the low-energy sector. Most importantly, quantum dynamics need not be ruled out despite the large $\boldsymbol{J}$ of the isolated RE^{3+} since the crystal-field Hamiltonian $H_{\rm cf}$ entangles a superposition of the $|m_J\rangle$ eigenstates of J^z.[23] As a result, $H_{\rm int}$, by virtue of its lack of commutation with $H_{\rm cf}$, can, in principle, have nonzero matrix elements between $|\psi^+\rangle$ and $|\psi^-\rangle$ and induce quantum dynamics within the low-energy Hilbert space spanned by $\prod_i^N |\psi_i^+\rangle|\psi_i^-\rangle$.

In $4f$ ions with an even number of electrons (i.e., non-Kramers ion) such as Pr, Tb, and Ho, time-reversal symmetry imposes that $\langle\psi^\pm|J^\pm|\psi^\mp\rangle = 0$.[24] Consequently, in presence of solely bilinear interactions of the form $K_{ij}^{uv}(r_{ij})J_i^u J_j^v$ with anisotropic K_{ij}^{uv} couplings, non-Kramers ions would display no quantum dynamics at low-energy and behave as effective $S = \frac{1}{2}$ classical Ising spins, as in the well-studied $LiHoF_4$ dipolar Ising system.[25] In the $(Pr,Tb,Ho)_2(Ti,Sn,Zr)_2O_7$ materials,[26] interactions beyond bilinear ones or consideration of the excited crystal-field states are necessary to cause quantum dynamics within the low-energy sector.[27–29] In that context, multipolar interactions in $Pr_2(Sn,Zr,Ir)_2O_7$ compounds[29] and virtual crystal-field excitations in the $Tb_2(Ti,Sn)_2O_7$ materials have been discussed.[27,28] Conversely, odd-electron (Kramers) ion systems (e.g., Gd, Dy, Er, Yb) are, in principle, symmetry allowed to have nonzero $\langle\psi^\pm|J^\pm|\psi^\mp\rangle$ matrix elements. The famous $Dy_2Ti_2O_7$ spin ice compound, in which the Dy^{3+} ions are Kramers ions and for which the excited crystal-field states lie at $\sim$300 K above the ground doublet,[30,31] has been shown to be well described by a dipolar spin ice model[32,33] with classical Ising spins.[3] This success very likely signals rather negligible interactions among the J_i^u components beyond bilinear ones, concomitantly with the specific spectral decomposition of $|\psi^\pm\rangle$ for Dy^{3+} in $Dy_2Ti_2O_7$.[30,31,34] On the other hand, $Er_2Ti_2O_7$ and $Yb_2Ti_2O_7$ have been known for some time[6,31,34] to have predominant "transverse" $\langle\psi^\pm|J^\pm|\psi^\mp\rangle$ matrix elements,[24] along with a non-negligible $\langle\psi^\pm|J^z|\psi^\pm\rangle$ "longitudinal" (g_{zz} tensor) component. Yet, the two compounds display quite different behaviors. $Er_2Ti_2O_7$ has overall antiferromagnetic interactions and develops long-range order at 1.2 K with zero propagation vector $\boldsymbol{q}_{\rm ord}$ and zero magnetic moment per tetrahedron[6] that is very likely induced by an order-by-disorder mechanism.[7] In contrast, $Yb_2Ti_2O_7$ has overall ferromagnetic interactions and exhibits a phase transition at $T_c \sim 0.24$ K.[35,36] However, the nature of the long-range order below T_c remains disputed[37–41] and the high sensitivity of the properties in the low-temperature regime ($T \lesssim 300$ mK) on sample quality is just beginning to be understood.[42–44] It is here, within the $Yb_2M_2O_7$ family[35,45] with overall ferromagnetic interactions and significant $\langle\psi^\pm|J^\pm|\psi^\mp\rangle$ matrix elements,[20,24] that the potential for an exotic class of quantum spin liquid arises,[21] a possibility that may have been casually dismissed from the naive perspective of "there should be negligible quantum effects in such large $\boldsymbol{J}$ rare-earth systems."

B. Quantum spin ice and $Yb_2Ti_2O_7$

The $Dy_2(Ti,Sn,Ge)_2O_7$ and $Ho_2(Ti,Sn,Ge)_2O_7$ pyrochlore oxide materials, along with the $CdEr_2Se_4$ spinel,[46] are classical Ising systems which may be viewed in their spin ice regime as collective paramagnets[47] or, employing a more contemporary terminology, classical spin liquids.[1] As discussed above, highly frustrated magnetic systems, by virtue of their low propensity to develop classical long-range order, are attractive candidates to search for quantum spin liquid behavior. Spin ice, reinterpreted as a classical spin liquid,[1] may thus be viewed as a natural setting to explore how the addition of quantum dynamics may give rise to a quantum spin liquid state. Such a topic was originally explored by Hermele, Fisher, and Balents[48] and Castro-Neto, Pujol, and Fradkin[49] a few years ago in the context of minimal theoretical models. These two groups argued in their respective papers that the addition of quantum dynamics within a parent (constrained) classical spin ice manifold may promote the system to a U(1) quantum spin liquid. Such a state would be describable by a quantum field theory analogous to that of quantum electrodynamics (QED) in $3 + 1$ dimensions. As a consequence, this U(1) spin liquid state would display "electric" and "magnetic" charge excitations and an accompanying gauge boson, or "artificial photon."[48,49] Numerical simulations have, over the past few years, suggested that such phenomenology may indeed be at play in various lattice models.[50,51] Such a U(1) quantum spin liquid state, which may be referred to as "quantum spin ice,"[27] has been suggested to explain some of the properties of real materials such as $Tb_2Ti_2O_7$ (Refs. 27 and 28) and

$Pr_2(Sn,Zr)_2O_7$.[29] Most recently, it has been proposed that Yb-based $Yb_2M_2O_7$ pyrochlore oxides[20,21] may offer an exquisite class of systems to investigate the possible existence of a quantum spin ice state and where the complexities of virtual crystal-field fluctuations[27,28] and magnetoelastic coupling[52,53] that complicate the $Tb_2(Ti,Sn)_2O_7$ compounds are avoided. In a theory paper building on the original work of Hermele *et al.*,[48] Savary and Balents have recently put forward a mean-field lattice gauge theory[21] which identifies a number of possible phases, the most exotic ones being the aforementioned U(1) spin liquid[48,49] as well as a novel Coulomb ferromagnet state. This approach has been further extended to non-Kramers ion systems.[22] Finally, the question of how to probe the emergent photon in a quantum spin ice via inelastic neutron scattering measurements has been recently discussed.[54]

One particularly interesting aspect of the search for quantum spin liquids in the Yb-based pyrochlores, and perhaps Pr-based pyrochlores as well,[22,29,55] is that the microscopic Hamiltonian is parametrized by a handful of independent anisotropic exchange parameters $\{J_e\}$ (four for Yb^{3+} and three for Pr^{3+})[20,22,56–58] between effective spin-$\frac{1}{2}$ degrees of freedom on each pyrochlore lattice site. Furthermore, it may be that the long-range dipolar interactions, so important in classical $Dy_2(Ti,Sn)_2O_7$ and $Ho_2(Ti,Sn)_2O_7$ spin ices with the large magnetic moment (10 μ_B) of Dy^{3+} and Ho^{3+},[3,11,32,33,59,60] can perhaps be neglected as a first approximation. To make definite progress at this time, a determination of the effective anisotropic exchange from experiments and theory that uses controlled approximations is required in order to position a candidate spin ice material in the phase diagram of Ref. 21, or the corresponding phase diagram relevant to non-Kramers ions.[22] In the case of $Yb_2Ti_2O_7$, the determination of those interactions from a series of experiments[20,34,40,56,61,62] has led to different $\{J_e\}$ sets with very different numerical values. Perhaps most noteworthy, a determination of those parameters from a fit to spin waves in strong magnetic field measured via inelastic neutron scattering[20] gives values significantly different than those obtained by fitting the zero-field diffuse paramagnetic neutron scattering using a random phase approximation (RPA) method[56] at a temperature $T \sim 1.4$ K or a subsequent polarized neutron scattering version, also using RPA as the fitting procedure, but now very near T_c.[40] Encouragingly, however, recent numerical linked-cluster (NLC) calculations[63] have found the zero-field magnetic specific heat data of $Yb_2Ti_2O_7$ to be well described above 0.7 K by the $\{J_e\}$ set obtained from the inelastic neutron scattering,[20] but not by the other sets determined from RPA fits to diffuse neutron scattering.[40,56]

It is clearly desirable to fit bulk measurements to determine the $\{J_e\}$ parameters in cases where inelastic neutron scattering studies are impractical, and to corroborate such neutron studies and understand thermodynamic and bulk magnetic properties in a common framework with neutron studies whenever possible. Yet, the scarcity of controlled numerical methods readily available to calculate the thermodynamic properties of frustrated three-dimensional anisotropic quantum spin systems in a temperature regime where nontrivial correlations develop does not make this task straightforward. With the seeming success of previous NLC calculations applied to $Yb_2Ti_2O_7$,[63] we are thus naturally led to ask the following broader question: *Can one convincingly demonstrate that NLC does provide a controlled method to describe bulk data for a three-dimensional frustrated quantum (spin ice) system as it progressively enters its low-temperature strongly correlated regime?*

In this paper, we address this question by extending the work of Ref. 63 by computing the thermodynamic properties of $Yb_2Ti_2O_7$ in nonzero magnetic field using NLC and by comparing the results of such calculations with measurements above 2 K on single crystals. We show, through a comparison with NLC, that the effective Hamiltonian with its anisotropic exchange parameters $\{J_e\}$ previously determined by fitting spin waves in the field polarized paramagnetic state[20] describes, with no adjustment, the temperature T and magnetic field h dependence of the magnetization $M(T,h)$ of $Yb_2Ti_2O_7$. As a consequence, we demonstrate simultaneously the usefulness of the NLC method and further validate[63] the quantitative merit of the effective spin Hamiltonian of Ref. 20 to describe $Yb_2Ti_2O_7$.

The rest of the paper is organized as follows. In the next section, we describe the effective spin-$\frac{1}{2}$ model for $Yb_2Ti_2O_7$ along with the NLC method. In Sec. III, we discuss the details of the experimental method employed. The NLC results are presented in Sec. IV, while Sec. V provides a comparison between experiment and theory. A brief discussion in Sec. VI concludes the paper.

II. MODEL AND COMPUTATIONAL METHOD

Symmetry considerations imply that nearest-neighbor bilinear exchange constants on the pyrochlore lattice can be parametrized in terms of four distinct exchange parameters $\{J_e\}$ and two g factors. In the local basis, this model is defined by the Hamiltonian[20,21,55]

$$\begin{aligned}\mathcal{H}_{\rm QSI} = \sum_{\langle i,j\rangle} \big\{ & J_{zz} S_i^z S_j^z - J_{\pm}(S_i^+ S_j^- + S_i^- S_j^+) \\ & + J_{\pm\pm}[\gamma_{ij} S_i^+ S_j^+ + \gamma_{ij}^* S_i^- S_j^-] \\ & + J_{z\pm}\big[S_i^z(\zeta_{ij} S_j^+ + \zeta_{i,j}^* S_j^-) + i \leftrightarrow j\big]\big\}. \end{aligned} \quad (1)$$

Several notation conventions are possible for $\mathcal{H}_{\rm QSI}$.[20,56–58] Here, we adopt the one used in Ref. 20. In Eq. (1), $\langle i,j\rangle$ refers to nearest-neighbor sites of the pyrochlore lattice, γ_{ij} is a 4×4 complex unimodular matrix, and $\zeta = -\gamma^*$.[20,21] The $\hat{z}$ quantization axis is along the local [111] direction,[23] and $\pm$ refers to the two orthogonal local directions. The $\overleftrightarrow{g}$ tensor takes eigenvalues g_{zz} along the local [111] cubic direction and g_{xy} perpendicular to it.[23,24] In the presence of an applied external magnetic field $\boldsymbol{h}$, an additional Zeeman interaction $H_Z = -\boldsymbol{h}\cdot\overleftrightarrow{g}\cdot\boldsymbol{S}\mu_B$ is added to $\mathcal{H}_{\rm QSI}$, giving a total spin Hamiltonian $\mathcal{H} = \mathcal{H}_{\rm QSI} + \mathcal{H}_Z$.

According to conventional mean-field theory[20] and a recent gauge mean-field theory (g-MFT),[21] the Hamiltonian (1) displays in the $J_{z\pm}/J_{zz}$ versus $J_{\pm}/J_{zz}$ ($J_{\pm\pm}=0$) plane two semiclassical long-range ordered phases: an antiferromagnetic phase and a "splayed ferromagnetic" (*sp*-FM) one. The *sp*-FM phase shares, as we will see later, some similarities with the behavior of the model (1) for the values $\{J_e\}$ we consider for $Yb_2Ti_2O_7$. In the *sp*-FM phase, each primitive tetrahedron unit has the same magnetic moment configuration

($\boldsymbol{q} = 0$ ordering wave vector) with the magnetization pointing along one of the cubic $\langle 100 \rangle$ axes. The g-MFT also predicts two exotic intrinsically quantum states. The U(1) spin liquid phase already exposed in Refs. 48 and 49 and a new "Coulomb ferromagnet" (CFM) phase which has a nonzero magnetization but deconfined spinon excitations.

As already stated above, there have been several experimental attempts to determine these $\{J_e\}$ effective exchange parameters leading to widely different results.[20,34,40,56,61,62] Among them, Ross *et al.*[20] used inelastic neutron scattering (INS) data obtained from measurements in high magnetic fields (i.e., in the polarized paramagnetic state) to determine the $\{J_e\}$ couplings for $Yb_2Ti_2O_7$: $J_{zz} = 0.17 \pm 0.04$, $J_{\pm} = 0.05 \pm 0.01$, $J_{\pm\pm} = 0.05 \pm 0.01$, and $J_{z\pm} = -0.14 \pm 0.01$, all in meV and with $g_{zz} = 1.80$ and $g_{xy} = 4.32$. In a recent numerical study,[63] it was found that the zero-field specific heat and entropy deduced from the data of Blöte *et al.*[36] are well described only by the exchange parameters obtained by Ross *et al.*[20] A key goal of this paper is to investigate further the validity of the Hamiltonian (1) as a description of the bulk properties of $Yb_2Ti_2O_7$ with the $\{J_e\}$ exchange couplings from Ref. 20. We do so by performing calculations of the thermodynamic properties of model (1) as a function of temperature T and magnetic field h and compare the numerical results with those obtained from experimental measurements. We find an excellent agreement without any adjustment of the parameters determined by Ross *et al.*,[20] hence providing a strong validation to the $\{J_e\}$ parameters determined by INS. As a corollary, our work confirms that fitting the INS spectra at high magnetic field is an excellent method to determine the exchange constants for pyrochlore oxides with well-isolated magnetic ground doublets and which are well described by an effective spin-half model.[55] Further implications of this agreement will be discussed in the concluding Sec. VI.

To calculate the thermodynamic properties of model (1), we turn to numerical linked-cluster (NLC) expansions.[64] In this method, an extensive property P (such as heat capacity or magnetization) of a thermodynamic system is calculated as a sum over contributions from different clusters embedded in the lattice:

$$P/N = \sum_c L(c) \times W(c). \tag{2}$$

Here, $L(c)$ is the count of the cluster per lattice site, defined as the number of ways to embed the cluster. $W(c)$ is the weight of the cluster which is obtained by calculating the property for a given cluster and subtracting the weight of all its subclusters

$$W(c) = P(c) - \sum_s W(s). \tag{3}$$

Here, the sum $\sum_s$ runs over all subclusters of the cluster c, where a subcluster is defined as any cluster smaller than c that can be embedded in cluster c. This scheme can be used to develop power series expansions, such as high-temperature series expansions in powers of inverse temperature β or some coupling constant expansion (such as expansion in inverse field strength). It can also be used to numerically calculate properties for a given value of temperature and coupling constants, as we do in this work.

The pyrochlore lattice is a lattice of corner-sharing tetrahedra and it proves useful to develop NLC in terms of clusters consisting of complete tetrahedra. We have calculated temperature and field-dependent properties up to fourth order, that is, including contributions from all clusters made of up to four tetrahedra. These NLC calculations are numerically exact in two limits. They are so at high temperatures since corrections to fourth-order NLC is of order β^6 in the high-temperature series expansion for $\ln Z$, where Z is the partition function. The NLC calculations are also exact at high magnetic field h at all temperatures since corrections to fourth-order NLC for $\ln Z$ is of order $(J/h)^5$ at $T = 0$ with exponentially small corrections $\exp(-\alpha h/T)$ at finite temperatures (α is some h- and T- independent constant). The parameter region where NLC begins to lose accuracy is when the temperature and the applied field (Zeeman energy) are both smaller than the exchange constants. We return to this matter in more detail when presenting the T and h dependencies of the specific heat $C(T,h)$ and entropy $S(T,h)$ in Sec. V C (Figs. 6 and 7). Thus, as long as either the high-temperature expansion or the high-field expansion converges, the NLC calculations should be accurate.

The reason for developing NLC in terms of complete tetrahedra comes from the fact that, for spin ice systems, the "ice rule" constraints at the origin of spin ice physics are local to tetrahedra. Thus, having clusters with only parts of a tetrahedron would cause wild oscillations in the calculated properties as the constraints can not be satisfied for such a cluster. Having only clusters with full tetrahedra allows the system to always satisfy the ice rule constraint. For example, in the case of the classical nearest-neighbor spin ice exchange model, such a tetrahedra-based NLC was found to be highly accurate.[65] In fact, the first-order NLC, which uses a single tetrahedron and is equivalent to Pauling's approximation for the entropy of ice, gives quantities at all temperatures (in zero external field) that are accurate to a few percent.[65]

However, in the quantum spin ice problem, NLC must break down at low temperatures due to the development of either long-range correlations or long-range entanglement. We have found (see results below and in Ref. 63) that the first signature of such a breakdown in the low-temperature and low-field regions is an alternation of the thermodynamic property P considered. This reflects the fact that, as system sizes increase, the thermodynamic properties must approach their infinite-size values in some way. Now, imagine that, at some order, the numerically calculated property is a bit too large, giving rise to a large cluster weight $W(c)$. Subcluster subtraction then causes the weight in the subsequent order to be too small. This, in return, causes an alternation with the NLC order considered in the property obtained when restricting the sum to some order. Such an alternation is handled well by using the Euler summation method,[66] which ensures that an alternating piece is completely eliminated from the partial sums at all orders. Thus, the Euler resummed properties are only missing the longer-range correlations which are necessarily absent in finite-order NLC. For $Yb_2Ti_2O_7$, we have found that in zero magnetic field[63] the thermodynamic properties converge down to 2 K without the Euler summation and down to about 1 K with Euler summation [the largest exchange constant for $Yb_2Ti_2O_7$, J_{zz} in Eq. (1), being approximately 2 K (Ref. 20)].

A. Computational details

NLC using the tetrahedral basis requires exact diagonalization of increasingly larger tetrahedral clusters. Using a single Intel® Core™ i7-920 processor and freely available LAPACK linear algebra routines, diagonalizations for clusters of one tetrahedron (four sites) and two tetrahedra (seven sites) could be done in less than a second, while the three-tetrahedron (10-site) cluster still required less than 10 s. Computing only the spectrum for a single four-tetrahedron (13-site) cluster required approximately 25 min of CPU time and 2.1 GB of memory, or slightly over twice the memory required to store the full Hamiltonian matrix (2^{26} complex numbers). Generating the full set of eigenstates required between 4 and 8 GB of memory. With the computer resources available to us, full exact diagonalization of larger systems, and thus higher orders of NLC expansion, were prohibited by memory requirements.

A list of different topological clusters with complete tetrahedra is shown in Fig. 1. A single site must be treated as a cluster as well, but is not shown. Because the local quantization $\hat{z}$ axis varies from sublattice to sublattice in the $RE_2M_2O_7$ pyrochlore oxides,[5,23] in the presence of a magnetic field, each cluster with different types of sublattice site must be treated separately. For example, each of the four single-site graphs (in NLC order $n = 0$) must be treated separately for a general field direction. A single tetrahedron graph remains unique even in a field. But, the graph with two tetrahedra joined at a vertex (NLC order $n = 2$) is really four distinct graphs that depend on the type of site (i.e., sublattice) that is shared between the two tetrahedra. Similarly, all higher-order graphs must be split into several distinct graphs to complete the calculation.

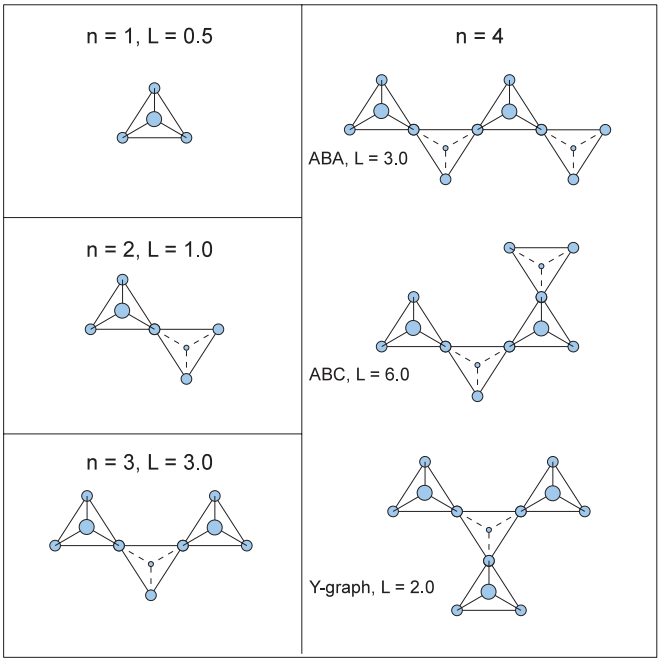

FIG. 1. (Color online) List of topological clusters with complete tetrahedra. In an applied field, each cluster must be treated as several distinct clusters as explained in the text. The integer n refers to the order at which the cluster arises and L gives the cluster count in zero field.

1. Calculation of observables

We use the eigenvalue spectrum $\{E_\alpha\}$ of $\mathcal{H} = \mathcal{H}_{\rm QSI} + \mathcal{H}_{\rm Z}$ to compute the partition function Z:

$$Z = \mathrm{Tr}(e^{-\beta\mathcal{H}}) = \sum_\alpha e^{-\beta E_\alpha}. \tag{4}$$

The expectation value for the internal energy is computed from the formula

$$E = \langle\mathcal{H}\rangle = \mathrm{Tr}(\mathcal{H}e^{-\beta\mathcal{H}})/Z. \tag{5}$$

This quantity is used, in turn, to compute the entropy as

$$S/k_{\rm B} = \beta E + \ln Z, \tag{6}$$

to which the heat capacity is related as

$$C = T\frac{\partial S}{\partial T}. \tag{7}$$

The average magnetization per site $M(T,h)$ is calculated as a derivative of the free energy with respect to the applied magnetic field h:

$$M(T,h) = \beta^{-1}\frac{\partial}{\partial h}\ln Z. \tag{8}$$

In practice, an approximation of this derivative at a given field value requires two separate evaluations of the free energy separated by a small change of field strength, in this case 10^{-6} T.

We believe in the correctness of the results from our calculations of the field-dependent properties for the following three reasons. First, the same results were obtained from two independently written computer programs. Second, we checked that in the limit $h \to 0$, the zero-field results[63] were reproduced. Third, we checked that at high temperatures the weights of the clusters were found to scale with the expected powers of inverse temperature β. These powers can be deduced from considerations of a high-temperature expansion of the quantity of interest. Consider, for example, an expansion for $\ln Z$. In such an expansion, either at least two powers of $\beta \equiv 1/(k_{\rm B}T)$ arise for each tetrahedron or at least one power of β arises for each tetrahedron together with two powers of β from placing the Zeeman $\mathcal{H}_{\rm Z}$ field term on sites at the outside perimeter of the cluster, as needed to give a nonzero contribution to the trace in Eq. (4). Thus, the weight of the four-tetrahedra cluster is of order β^8 in zero field and of order β^6 in nonzero field. These latter checks are nontrivial and demonstrate that all subgraphs have been properly subtracted within the NLC procedure.

2. Euler summation

NLC generates a sequence of property estimates $\{P_n\}$ with increasing order n, where $P_n = \sum_{i=1}^{n} S_i$. The convergence of such a sequence can be improved by Euler summation.[63,66] In general, given alternating terms $S_i = (-1)^i u_i$, the precise infinite-size lattice property $P_\infty(\mathcal{L})$ is approached by the sum (with n even)

$$u_0 - u_1 + u_2 - \cdots - u_{n-1} + \sum_s^\infty \frac{(-1)^s}{2^{s+1}}[\Delta^s u_n], \tag{9}$$

where Δ is the forward difference operator

$$\begin{aligned}\Delta^0 u_n &= u_n,\\ \Delta u_n &= u_{n+1} - u_n,\\ \Delta^2 u_n &= u_{n+2} - 2u_{n+1} + u_n,\\ \Delta^3 u_n &= u_{n+3} - 3u_{n+2} + 3u_{n+1} - u_n, \ldots .\end{aligned} \tag{10}$$

Usually, a small number of terms are computed directly, and the Euler transformation, $P_{n,\mathrm{E}}$ defined below, is applied to the rest of the series. In our case, where direct terms were available up to fourth order, we began the transformation after the second order, so that the third- and fourth-order Euler-transformed property estimates $P_{3,\mathrm{E}}$ and $P_{4,\mathrm{E}}$, respectively, are given by

$$\begin{aligned}P_{3,\mathrm{E}} &= S_0 + S_1 + S_2 + \frac{1}{2}S_3,\\ P_{4,\mathrm{E}} &= P_{3,\mathrm{E}} + \frac{S_3 + S_4}{4}.\end{aligned} \tag{11}$$

III. EXPERIMENTAL METHODS

As we are aiming to establish a close connection between experiment and theory for the temperature and field dependence of the magnetization $M(T,h)$, it is necessary to perform adequate demagnetization corrections and this, in turn, necessitates measurements on single crystals. Magnetization experiments were thus carried out on three single-crystal pieces. The samples were cut from two large single crystals grown by the optical floating zone method, using a growth procedure similar to that previously employed for growing single crystals of $Tb_2Ti_2O_7$.[67] One crystal, which provided samples aligned along [110] and [100], was grown at a rate of 6 mm/h in oxygen pressure of 4 atm. The second crystal, from which a piece aligned along [111] was cut, was grown at 5 mm/h in 2 atm of oxygen. The samples were aligned using x-ray diffraction to within 2° of each of the three high-symmetry directions: [100], [110], and [111]. Two single-crystal samples were cut into rectangular prisms ("needles") measuring 0.74 mm × 0.74 mm × 3.74 mm and 0.69 mm × 0.65 mm × 2.67 mm, respectively, with [111] and [100] directions oriented along their long axes. The applied magnetic field was also oriented parallel to the long axis. The third single-crystal piece was cut and polished into a rounded triangular shape which we approximate, for the purposes of demagnetization corrections, as an ellipsoid with major axes $a = 1.85$ mm, $b = 1.5$ mm, and $c = 0.8$ mm. The a direction made an angle of 22° with respect to both [110] and the applied field direction within the ab plane. The magnetization of the same [110] sample was also reported in Ross *et al.*,[39] but without a demagnetization correction applied. The data were collected with a Quantum Design MPMS instrument, which uses a SQUID magnetometer to measure the dc magnetization in magnetic fields up to 5 T and temperatures as low as 1.8 K. The magnetization data for the [100] and [111] samples were corrected for demagnetization effects using an approximate formula for the demagnetization field in rectangular prisms.[68] The data for the [110] sample were corrected by approximating it as a very flat ellipsoid, with the field direction 22° from the (long) a direction. In general, the apparent susceptibility $\chi_A \equiv M(T,h)/h_{\mathrm{applied}}$ should be corrected to account for the demagnetization field using the following formula, in SI units:

$$1/\chi = 1/\chi_A - N, \tag{12}$$

where χ is the actual susceptibility that we aim to compare with the results $M(T,h)/h$ from NLC calculations. χ_A is the apparent susceptibility and N is the demagnetization factor, which depends on the sample geometry.[68]

IV. NLC RESULTS: THERMODYNAMIC PROPERTIES

The temperature dependence of the magnetization $M(T,h)$ divided by the strength of the applied magnetic field h along the cubic [100] direction and calculated using the NLC method is shown in Fig. 2. Figures 2(a) and 2(b) show the results for a field of 0.2 and 1.0 T, respectively. The experimental values of $M(T,h)/h$, after demagnetization corrections, are shown for the same applied field values and are marked by black pluses. The number beside each curve labels the NLC order at which $M(T,h)$ was calculated (see Sec. II). NLC-0 (red curve, label "0") considers a single-site cluster. It therefore

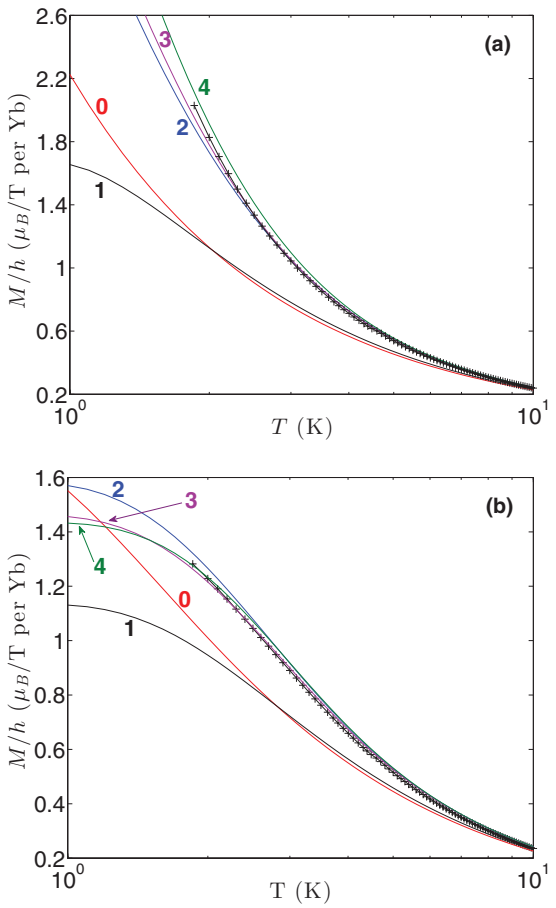

FIG. 2. (Color online) The figure illustrates the evolution of the magnetization divided by the field strength $M(T,h)/h$ with NLC order n and convergence towards the experimental data. Panels (a) and (b) are for $h = 0.2$ and 1.0 T, respectively, and with the field h applied along the [100] direction. Solid curves are for the NLC calculations and the number beside each curve corresponds to the order n up to which the calculations were carried out. Pluses are the demagnetization corrected experimental $M(T,h)$ results divided by h.

does not incorporate the effect of the interactions in Eq. (1) between the Yb^{3+} ions and thus corresponds to the Yb^{3+} single-ion property with g-tensor components $g_{zz} = 1.80$ and $g_{xy} = 4.32$. The significant differences between NLC-0 and the experimental data emphasize the importance of interactions and concurrent development of correlations below 10 K. The importance of interactions on causing a departure of $M(T,h)/h$ from its single-ion value below $T \lesssim 10$ K had previously been noted on the basis of a determination of the local susceptibility from polarized neutron measurements[61,62] as well as a subsequent theoretical calculation of the local susceptibility[69] using exchange parameters determined from RPA fits to the diffuse paramagnetic scattering.[56] However, none of these works[61,62,69] had the quantitative descriptive power of the present NLC calculations.

Compared to NLC-0, NLC-1 incorporates the effect of interactions and correlations at the scale of one tetrahedron (see Fig. 1). Focusing on the case $h = 0.2$ T, one observes little difference between NLC-0 and NLC-1 above $T \sim 2$ K, but a large increase in $M(T,h)/h$ in going from NLC-1 to NLC-2 for $T \lesssim 7$ K. The results for NLC-1 require the exact diagonalization of the Hamiltonian over a single tetrahedron and, therefore, incorporates spatial spin-spin correlations extending only over a nearest-neighbor distance (see panel for $n = 1$ in Fig. 1). In contrast, NLC-2 considers two tetrahedra (see panel for $n = 2$ in Fig. 1) and therefore considers correlations, and associated fluctuations, reaching out to third-nearest neighbors. As first noted by Ross *et al.*,[20] and further expanded upon by Applegate *et al.*,[63] the fluctuations of the joining spin/site of two tetrahedra mediate, via the $J_{z\pm}$ coupling in Eq. (1), an effective ferromagnetic third-nearest-neighbor coupling (J_3 in Ref. 63). This fluctuation-induced interaction promotes ferromagnetic correlations among the otherwise degenerate classical 2-in/2-out spin ice states, an effect that we believe important to induce ferrimagnetic correlations in $Yb_2Ti_2O_7$.[20,21,63] The incorporation of this fluctuation process and induced effective J_3 coupling only happens for NLC order $n \geqslant 2$ and is thus absent for NLC-1. We believe that the large increase of $M(T,h)/h$ in going from NLC-1 to NLC-2 results from the ability of clusters of two tetrahedra to support that type of fluctuation physics while a single tetrahedron can not. One may want to argue that the observed large increase of the calculated $M(T,h)/h$, when going from NLC-1 to NLC-2, is further evidence that $Yb_2Ti_2O_7$, as described by the effective exchange parameters of Ref. 20, is either on its way or at the verge of developing spontaneous ferrimagnetic order at low temperature. The current lack of consensus[35,37–41] about the ground state of $Yb_2Ti_2O_7$ below the $T_c \sim 0.26$ K transition[35,42–44] indicates that if this system does indeed have a tendency towards splayed ferromagnetic (*sp*-FM) order, this tendency is either interrupted at $T \gtrsim T_c$ or is quite fragile with respect to perturbations not included in the model (1). We return to this point below in Sec. V C when we discuss the magnetic entropy $S(T,h)$ in nonzero magnetic field h.

Considering the results of Fig. 2(a), we observe that the NLC-2, -3, and -4 results are quite close to each other down to $T \sim 1.8$ K, the lowest temperature available for the experimental data. Most importantly, one should note that NLC-2, -3, and -4, using the effective anisotropic exchange parameters $\{J_e\}$ of Ref. 20, already provide, without Euler summation, and *without any* adjustment of the parameters defining $\mathcal{H}_{\rm QSI}$ and $\mathcal{H}_{\rm Z}$, a very good agreement with the experimental data. A similarly good agreement is also found between the experimental data and the NLC results for the highest NLC orders ($n = 3,4$) for a field $h = 1$ T [see Fig. 2(b)].

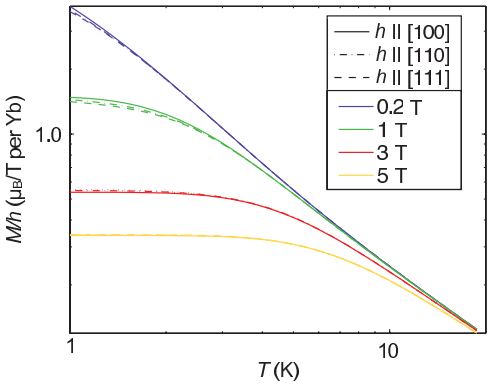

FIG. 3. (Color online) Calculated magnetizations as a function of temperature for different field strengths and directions are shown using the fourth-order Euler-transformed results from the NLC expansion [see. Eq. (10)]. The magnetic fields are applied along the [100], [110], and [111] directions.

Having demonstrated that (i) interactions do play a strong effect in renormalizing $M(T,h)$ for $T \lesssim 10$ K and that (ii) NLC orders $n = 3$ and 4 give a highly suitable description of the experimental data even for the weakest field $h = 0.2$ T considered (see the discussion in Sec. II), we henceforth solely report results from the Euler transformation method to order $n = 3$ and 4 [see Eqs. (10) and (11)] to generate theoretical values of $M(T,h)/h$ versus temperature and for various field h along the three high-symmetry cubic directions ([100], [110], and [111]).

Figure 3 shows $M(T,h)/h$, obtained using the fourth-order Euler-transformed NLC results, as a function of temperature T for fields h of strength 0.2, 1, 3, and 5 T oriented parallel to the [100], [110], and [111] directions. Again, the calculation employed the microscopic Hamiltonian appropriate to $Yb_2Ti_2O_7$ as derived from inelastic neutron scattering data at high field.[20] Figure 3 shows fourth-order NLC results for $M(T,h)/h$ per Yb^{3+} ion versus temperature T, with both quantities plotted on a log scale. The calculated magnetization is relatively independent of direction and levels off at low temperatures, with the temperature at which it levels off being lower with smaller applied magnetic fields. While the magnetization is only weakly dependent on the direction of the applied magnetic field, such differences in the magnetization as a function of direction of field are only evident at low temperatures.

V. MAGNETIZATION: CONFRONTING THEORY WITH EXPERIMENT

A. Field-dependent magnetization

Figure 4 shows the experimentally determined magnetization as a function of temperature on a semilog plot. Data are shown for applied magnetic field directions parallel to [100], [110], and [111], from top to bottom, and for field strengths

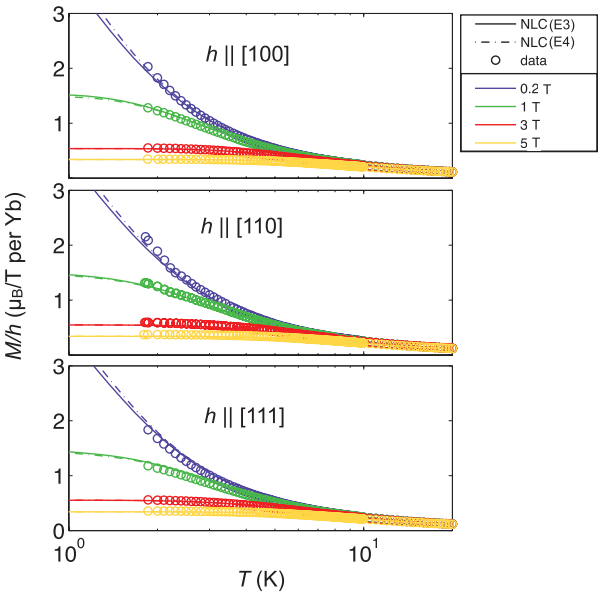

FIG. 4. (Color online) Calculated magnetizations using the $n = 3$ and 4 Euler-transformed $M(T,h)/h$ NLC expansion results [see Eq. (10)] are compared with the measured magnetization versus temperature for fields applied along the [100], [110], and [111] directions. The parameters for $\mathcal{H} = \mathcal{H}_{\rm QSI} + \mathcal{H}_{\rm Z}$ are those determined from the spin-wave results of Ref. 20. Appropriate demagnetization corrections have been applied to all experimental data. Departures between $n = 3$ and 4 NLC expansion results become noticeable at temperatures $T \lesssim 1.8$ K.

of 0.2, 1, 3, and 5 T. Once again, $M(T,h)/h$ is normalized per Yb^{3+} ion. Two sets of NLC expansion calculations using the Euler transformation are shown in Fig. 4; calculations to order $n = 3$ are shown as the solid lines and those to order $n = 4$ are shown as the dotted-dashed lines. Here again, the NLC expansions utilized the microscopic Hamiltonian derived from the high-field inelastic neutron scattering (INS) data[20] with no adjustment in the parameters so determined.

Several features are immediately clear from this comparison between theory and experiment. First, the (Euler-transformed) NLC expansion results to both $n = 3$ and 4 orders provide an excellent description of the magnetization for all field strengths and directions as well as all temperatures considered. The fact that a remarkable degree of quantitative agreement between theory and experiment is achieved without any adjustment of the microscopic Hamiltonian appropriate to $Yb_2Ti_2O_7$ is strong validation of the determination of the microscopic Hamiltonian.[20] As the INS measurements were performed at $T = 0.03$ K and applied magnetic fields of $h = 2$ and 5 T with h parallel to [110], while the magnetization measurements are performed for $T > 1.8$ K and fields $\leqslant 5$ T, it would thus appear that we now have a very accurate description of $Yb_2Ti_2O_7$ using the same microscopic Hamiltonian over a remarkably large region of its $h - T$ phase diagram. We return to this point in Sec. VI.

Looking at the Euler-transformed NLC expansion results for $n = 3$ (solid line) and 4 (dotted-dashed line) in Fig. 4, one can see that, as expected, the two calculations are quite consistent with each other for $T \gtrsim 1.8$ K, but depart from each other at lower temperatures. There is also a better agreement at lower temperatures between $n = 3$ and 4 NLC expansions for higher fields, independent of the direction of the applied magnetic field, as anticipated on the basis of the general arguments presented in Sec. II.

B. Other parametrizations of $\mathcal{H}_{\rm QSI}$

Apart from Ref. 20, there have been over the last four years a number of other studies[34,40,56,61,62] combining experiment and theory that were aimed at determining the strength of the anisotropic interactions in $Yb_2Ti_2O_7$. We believe that most of these studies, if not all, including Ref. 56 that was coauthored by one of us, are beset by significant drawbacks compared to the in-field inelastic neutron scattering measurements of Ross *et al.*[20] In fact, one might have wondered whether the anisotropic exchange parameters $\{J_e\}$ extracted in Ref. 20 in magnetic fields of 5 T might have suffered from large renormalization due to magnetoelastic effects. The good agreement between experimental and NLC results for zero magnetic field specific heat[63] and those presented in this paper for the temperature and magnetic-field-dependent magnetization $M(t,h)$ provide compelling evidence that such renormalization, if it exists, is well within the experimental uncertainty of the estimated $\{J_e\}$ parameters.[20] That being said, we now discuss each of the other works.

Cao *et al.* used polarized neutron diffraction to extract the local susceptibility tensor of a number of $RE_2Ti_2O_7$ pyrochlores, including $Yb_2Ti_2O_7$, in an applied external field of 1 T along the [100] crystallographic direction.[61,62] Their analysis was based on a mean-field theory that ignores the sublattice nature of the pyrochlore lattice and incorporates the effect of the local mean-field only via two independent coupling constants referred to as λ_z and $\lambda_\perp$. By construction, such an approach with two free parameters makes it difficult to extract the microscopic exchange parameters of the spin Hamiltonian with four $\{J_e\}$ parameters. Furthermore, as they do not comment on this, it is not clear that their data analysis took into account demagnetization effects. Malkin *et al.* reinvestigated the description of the bulk and local susceptibility of $RE_2Ti_2O_7$ compounds, but now starting from a microscopic formulation, and incorporating an adequate sublattice structure in their model as well as including demagnetization corrections.[34] In the case of $Yb_2Ti_2O_7$, they reported being unable to describe the longitudinal site susceptibility χ of Cao *et al.* by using a single set of crystal-field parameters. It is perhaps important to note that Malkin *et al.* assumed that the bilinear anisotropic interactions between the magnetic moment operators were symmetric, which amounts to neglecting Dzyaloshinskii-Moriya- (DM-) type interactions. This may have been partly responsible in causing difficulties for obtaining a quantitative description of this material.

Thompson *et al.*[56] were the first to consider a microscopic theory which incorporates the single-ion crystal-field Hamiltonian $H_{\rm cf}$ for Yb^{3+} in $Yb_2Ti_2O_7$, the four symmetry-allowed bilinear nearest-neighbor interactions, $K_{ij}^{\mu\nu}$ between the $\boldsymbol{J}_i$ angular momentum operators along with the long-range magnetostatic dipole-dipole interactions.[56] In order to determine the $K_{ij}^{\mu\nu}$ couplings, Thompson *et al.* used a random phase approximation to calculate the diffuse (energy-integrated) neutron scattering intensity $S(\boldsymbol{q})$ in the $[hhl]$ scattering phase

and compare with experimental measurements at a temperature $T_{\rm fit} = 1.4$ K.[70] With the Curie-Weiss temperature of $Yb_2Ti_2O_7$ given by $\theta_{\rm CW} \sim 0.5 \pm 0.2$ K, it would have seemed that RPA, which is in essence a mean-field scheme, may be *a priori* reasonably quantitatively accurate at a temperature $T = 1.4$ K with a frustration/fluctuation level set by $\theta_{\rm CW}/T \lesssim 0.3$. Forced by construction to describe short-range diffuse scattering, the RPA fit of Ref. 56 provided a set of couplings K_{ij}^{uv} allowing for a good fit of $S(\boldsymbol{q})$ and, by "retroactive consistency," a mean-field critical temperature $T_c^{\rm RPA} \sim 1.1$ K $< T_{\rm fit} = 1.4$ K. When translating the determined K_{ij}^{uv} parameters in the $\{J_e\}$ notation of Ross *et al.*, one finds a large difference between the two sets.[63] The authors of Ref. 40 commented in the Supplemental Material section of their paper that a possible reason for the failure of the model of Thompson *et al.*[56] to agree with the results of Ross *et al.*[20] is that the former work neglected multipolar interactions between the $\boldsymbol{J}_i$ operators beyond the considered bilinear ones. However, as discussed in the Supplemental Material of Ref. 56, such critique[40] would appear of little merit for the following reason. Thanks to the essentially total isolation of the Kramers crystal-field doublet of Yb^{3+} from the excited states, the projection onto the ground crystal-field doublet acts as an almost exact *invertible* unitary transformation of the $K_{ij}^{uv} J_{i,u} J_{j,v}$ interactions. This then provides for a one-to-one correspondence between the bilinear K_{ij}^{uv} couplings and the $\{J_e\}$ effective anisotropic exchange between effective spin-$\frac{1}{2}$ operators of Ross *et al.*[20] In other words, the bilinear $K_{ij}^{uv} J_{i,u} J_{j,v}$ model of Ref. 56 can be viewed as a "high-energy" model whose projection (with "correct" values of the K_{ij}^{uv} couplings) gives the $J_e S_i^u S_j^v$ interactions in the model of Eq. (1).[20]

Rather than being flawed for ignoring multipolar interactions, the difficulty with Thompson *et al.*'s results[56] can be readily understood on the basis of the mean-field theory results presented in Ref. 20. The mean-field $T_c^{\rm mf}$ determined using the $\{J_e\}$ parameters from Ref. 20 is approximately $T_c^{\rm mf} \sim 3.5$ K $> T_c^{\rm RPA}$. Such a high $T_c^{\rm mf}$ compared to the $T_{\rm fit} = 1.4$ K RPA fit of $S(\boldsymbol{q})$ means that the extracted K_{ij}^{uv} parameters from Ref. 56 suffer from a very significant and uncontrolled renormalization from thermal (and possibly quantum) fluctuations. Concerns that $T_{\rm fit} = 1.4$ K might have been too low for a quantitative RPA fit of $S(\boldsymbol{q})$ of $Yb_2Ti_2O_7$ and that fits of the higher temperature 9.1-K data[56] might have been more appropriate had been expressed in Ref. 70. Unfortunately, the diffuse signal at 9.1 K proved too weak to proceed. As demonstrated by Applegate *et al.* in their NLC calculations,[63] because of their renormalization, the anisotropic exchange parameters of Ref. 56 provide a poor description of the zero-field magnetic specific heat $C(T)$ of $Yb_2Ti_2O_7$.

Chang *et al.* most recently reported their own estimate of the exchange parameters for $Yb_2Ti_2O_7$.[40] They also employed an RPA scheme to fit the (polarized) neutron scattering intensity of the compound, but using an effective spin-$\frac{1}{2}$ model rather than the bilinear $K_{ij}^{uv} J_{i,u} J_{j,v}$ interactions plus $H_{\rm cf}$ as done by Thompson *et al.*[56] Perhaps believing in the incorrectness of the latter description (see discussion two paragraphs above), the authors of Ref. 40 passed over in the body of their paper the opportunity to offer a critique of Thompson *et al.*'s model. That said, with the published evidence from Ref. 20 that

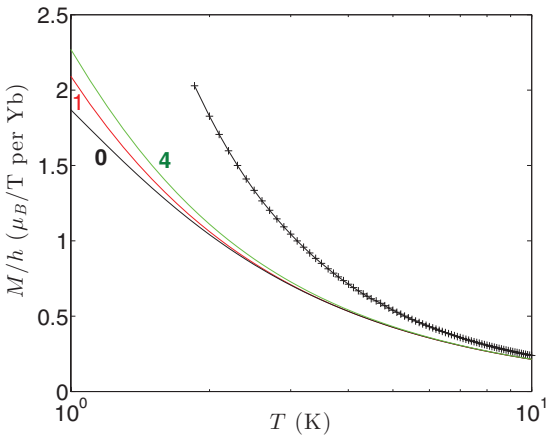

FIG. 5. (Color online) The figure shows that $M(T,h)$ from NLC calculations (orders $n = 0,1,4$) using the $\{J_e\}$ parameters reported by Chang *et al.* (Ref. 40) dramatically fail to describe the experimental $M(T,h)$ results (plus symbols). See text.

$T_c^{\rm mf}$ for $Yb_2Ti_2O_7$ may be as high as 3.5 K,[20] and that the RPA fits of Thompson *et al.* at $T_{\rm fit} = 1.4$ K may thus be of questionable quantitative merit, it is surprising that Chang *et al.* did nevertheless proceed to use RPA to fit the polarized neutron scattering at a temperature as low as 0.3 K, which is a mere 25% higher than the experimental $T_c \sim 0.24$ K. It is also not clear how the authors of Ref. 40 find a similarity between their $\{J_e\}$ values and those of Ross *et al.*, especially after evidence had been reported by Applegate *et al.*[63] that the $\{J_e\}$ of Ref. 40 fail to describe the magnetic specific heat $C(T)$, while those of Ross *et al.* provide a quite adequate description of $C(T)$.[63] Chang *et al.* propose a rationalization of the low-temperature state of $Yb_2Ti_2O_7$ on the basis of a Higgs-type phase and suggest positioning this material in a $\{J_e\}$ parameter space near a parent classical spin ice. Yet, at the same time, they overlook to comment on the inability of their microscopic model with its RPA-determined set of $\{J_e\}$ to describe $C(T)$.[63] As in the case of Thompson *et al.*'s RPA analysis,[71] Chang *et al.*'s fit to the neutron scattering data provides, by the very consequence of using RPA at a temperature T, with $T_c \ll T \ll T_c^{\rm mf}$, for a set of coupling parameters which are significantly and uncontrollably renormalized downward compared to the bare $\{J_e\}$. This is illustrated in Fig. 5 where it is shown that NLC-1 and NLC-4 using the $\{J_e\}$ parameters of Chang *et al.* do not describe $M(T,h)$ for temperatures $T \lesssim 10$ K, where correlations have barely started to develop.[56] In fact, down to $T = 1$ K, there is little difference between either NLC-1 and NLC-4 with the single-ion magnetization with all interactions turned off and given by the NLC-0 results.

To conclude this discussion, it thus appears that only Ross *et al.*'s set of microscopic parameters[20] consistently describe $Yb_2Ti_2O_7$ for fields $h < 5$ T and temperatures $T \gtrsim 0.7$ K. We return to this in Sec. VI.

C. Field-dependent specific heat

While we are not aware of in-field specific heat $C(T,h)$ measurements on $Yb_2Ti_2O_7$ single crystals, we expect these to be soon carried out given the interest devoted to this compound. One perspective as to why such measurements

might be of interest is the following. The $Er_2Ti_2O_7$ pyrochlore antiferromagnet displays a transition to long-range order at $T_c \sim 1.2$ K.[6,72,73] The application of a magnetic field along [110] ultimately destroys that order at $T = 0$, giving rise to a quantum phase transition at $h_c \sim 1.5$ T.[72,73] Specific-heat measurements in nonzero field have been found useful to characterize the evolution of this system in and out of the long-range-ordered phase at $h \lesssim 1.5$ T and $T \lesssim 1.2$ K.[72,73]

Measurements of $C(T,h)$ in $Yb_2Ti_2O_7$ for $T < 0.3$ K may thus well be very interesting. This would be especially true if, once the sample dependence of T_c has been understood and, if $T_c = 0.26$ K does indeed turn out to be a phase transition to a ferrimagnetically ordered state, as suggested by some experiments[40] and theory,[20,21,63] but not all experiments.[35,41,74] Thus, in anticipation that such measurements may be performed on $Yb_2Ti_2O_7$, we have used NLC expansion to calculate $C(T,h)$.

The specific heat $C(T,h)/R$ (R is the molar gas constant), calculated using the Euler-transformed NLC expansion to order $n = 4$ and the microscopic Hamiltonian determined for $Yb_2Ti_2O_7$ from inelastic neutron scattering (Ref. 20) is shown in Fig. 6. We present results for $C(T,h)/R$ for a field parallel to [100], [110], and [111] from top to bottom, respectively. In all cases, calculations are presented for field strengths ranging from 0.2 to 5 T. The magnetic entropy $S(T,h)$ results are shown in Fig. 7, with the same sequence of field magnitude and directions as in Fig. 6.

The curves of Fig. 6 show significant departure between the Euler-3 (E3) and Euler-4 (E4) results at temperatures $T \lesssim 1$ K for the lowest field of 0.2 T, accompanied by

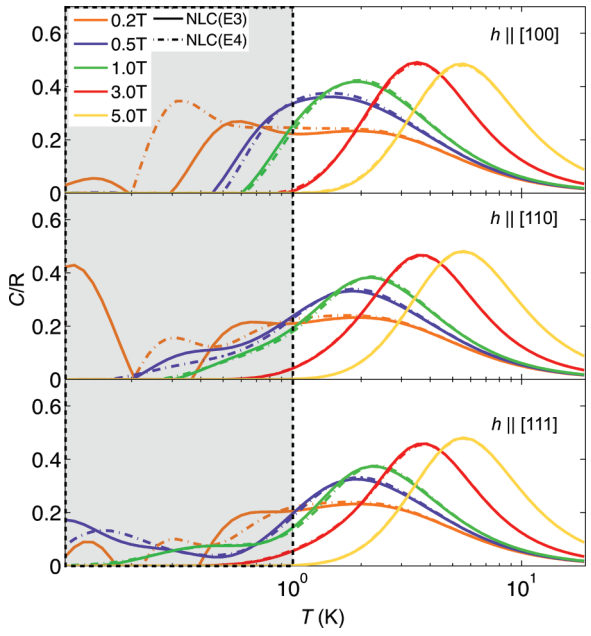

FIG. 6. (Color online) The calculated molar specific heat using NLC is shown as a function of temperature and magnetic field with field applied along, from top to bottom, the [100], [110], and [111] directions. These results were calculated using the $n = 3$ and 4 Euler transformation NLC results using the $\{J_e\}$ parameters of Ref. 20. The shaded region at low temperatures and fields indicates the regime where accurate NLC results are not available, as described in the text.

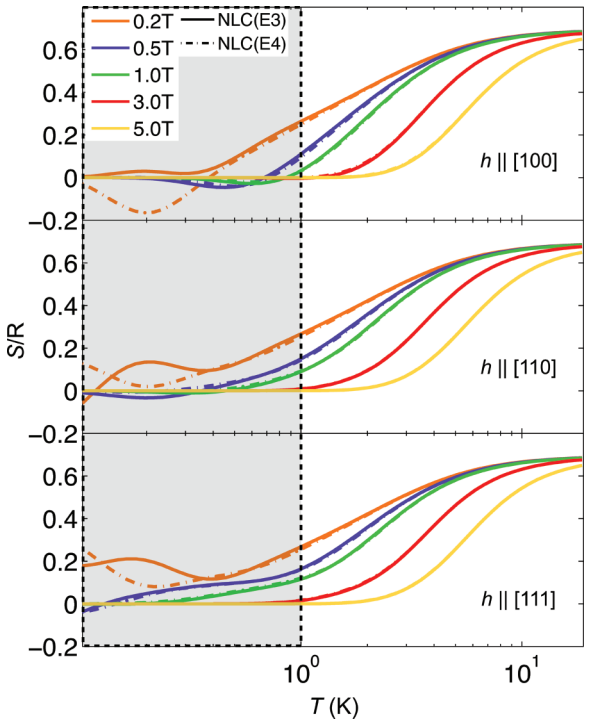

FIG. 7. (Color online) The calculated molar entropy using NLC is shown as a function of temperature and magnetic field with field applied along, from top to bottom, the [100], [110], and [111] directions. These results were calculated using the $n = 3$ and 4 Euler transformation NLC results using the $\{J_e\}$ parameters of Ref. 20. The shaded region at low temperatures and fields indicates the regime where accurate NLC results are not available, as described in the text.

$C(T)$ becoming negative for a certain temperature window. This is a nonphysical behavior and a consequence of the truncation of the NLC at order $n = 4$ and the neglect of correlations that would be supported by clusters of larger size than NLC-4 considers (see Fig. 1). Specific-heat results below $T \sim 1$ K should probably be viewed as inaccurate while the entropy $S(T,h)$ results are perhaps accurate at 0.2 T down to a slightly lower temperature ($T \sim 0.7$ K).[63] We identify, somewhat conservatively, the range $T < 1$ K where results become inaccurate by a shaded gray region in Figs. 6 and 7. As discussed in Sec. II, the lowest temperature at which the NLC results become numerically accurate decreases as the magnetic field h increases, as can be seen in Figs. 6 and 7 when the E3 and E4 results agree.

The trend in the specific-heat data of Fig. 6 is very similar for all three field directions. A broad peak is observed for a field strength h above ~2 T, with the peak position moving to lower temperatures as h is decreased. While the NLC calculation is inaccurate for temperatures less than ~1 K (see Ref. 63) and for appropriately low-field strengths, the calculated molar specific heat at the lowest applied magnetic fields is qualitatively consistent with that observed experimentally in zero field,[36] which shows a sharp anomaly at very low temperatures as well as a broad shoulder near 2 K.

Even though, at first sight, the thermodynamic properties look independent of the field direction, there are subtle differences at low temperatures and fields, which could be taken as evidence, at least in the model, of an ultimate

spontaneous ferrimagnetic ordering with M along [100] in zero field.[20,21,40,63,74] On close inspection, one finds that for fields of 1 T and lower, $C(T,h)$ is higher at temperatures around 1 K for the [100] direction and, as a result, the entropy $S(T,h)$ is substantially lower. In fact, as shown in Fig. 7, the entropy for fields $h = 0.5$ and 1 T along [100] appears to become vanishingly small at temperatures $T \lesssim 0.8$K, whereas there remains a residual entropy along the other two directions. The residual entropy remains largest along the [111] direction. This observation is consistent with the picture of a zero-field ordering in this system, characterized by $\boldsymbol{M}$ along one of the $\langle 100 \rangle$ crystallographic directions.[20,21,40,63] In that case, applying a field along [100] selects one ordered state and the system merely exhibits a crossover to a paramagnetic state at a temperature of order 1 K. The entropy then displays an activated temperature dependence at low temperatures. In contrast, for small fields along [110], two degenerate ordered states remain while three degenerate states remain for small fields along [111]. Thus, there should continue to be a low-temperature phase transition in sufficiently weak magnetic fields along either [110] or [111], with only below the transition the entropy going to zero. By its nature, NLC does not allow for our theoretical calculations to converge at low enough temperatures and magnetic fields to fully confirm this picture. It would thus be interesting to investigate its validity via experimental $C(T,h)$ measurements.

To summarize, for the model of Eq. (1) that we consider for $Yb_2Ti_2O_7$, the rather large anisotropic exchange interactions lead to the development of a collective paramagnetic state at $T < T_c^{\rm mf} \sim 4$ K with $\theta_{\rm CW} \ll T_c^{\rm mf}$, being thus somewhat "hidden" and difficult to quantitatively describe using standard textbook (e.g., RPA and other mean-field-like) methods. In this material, and perhaps in other candidate quantum spin ice materials,[35] the fit of bulk thermodynamic data such as $M(T,h)$ and $C(T,h)$ using NLC may provide a useful alternative to parametrize their spin Hamiltonian.

VI. DISCUSSION AND CONCLUSION

In this paper, we have compared the results from numerical linked-cluster (NLC) calculations of the temperature and magnetic-field-dependent magnetization of $Yb_2Ti_2O_7$ with those obtained from experimental measurements on this material in a temperature range $T \in [1.8,20]$ K and magnetic field range $h \in [0.2,5]$ T. The NLC calculations were performed on a Hamiltonian describing the interactions between pseudospins $S = \frac{1}{2}$ and characterized by effective anisotropic exchange couplings determined via inelastic neutron scattering (INS) measurements in the polarized paramagnetic state of $Yb_2Ti_2O_7$.[20] The overall agreement between the NLC and the experimental results were found to be excellent (see Fig. 4). Conversely, NLC magnetization results obtained using the exchange couplings determined from a random phase approximation analysis of the diffuse paramagnetic neutron scattering[40,56,71] were found to be in significant disagreement with the experimental magnetization measurements. The excellent agreement between NLC and experimental measurements of $M(T,h)$, down to a temperature of about 1 K, indicate that (i) the proposed nearest-neighbor exchange model[20] is quantitatively accurate to describe $Yb_2Ti_2O_7$, that (ii) high-field inelastic scattering in the polarized paramagnetic state is a reliable method for extracting effective exchange parameters, and that (iii) long-range dipolar interactions appear to not play an important role in the energetics of the system. The latter conclusion is perhaps a bit surprising given that long-range dipolar interactions play a key role in the physics of classical (dipolar) spin ices.[32,59,60] One obvious difference is that, relative to the J_{zz} effective exchange interaction, the nearest-neighbor contribution of the magnetostatic dipole-dipole interactions in $Yb_2Ti_2O_7$ is approximately one order of magnitude smaller than in the classical dipolar spin ices.[11,16,32,33] At the very least, one may consider that the nearest-neighbor contributions of the dipolar interactions are "already" incorporated in the $\{J_e\}$ effective anisotropic exchange. Then, it thus appears that the perturbative long-range (beyond nearest-neighbor) part of the dipolar interactions plays no dramatic role in a field greater than 0.2 T and down to 1.0 K (Figs. 6 and 7) or, in zero field, down to approximately 0.7 K as found in Ref. 63. It may be that, if $Yb_2Ti_2O_7$ does indeed possess a splayed ferromagnetic ordered state with a magnetization along the $\langle 100 \rangle$ axes, as suggested by some studies,[37,40] that the sole role of dipolar interactions is to weakly renormalize the critical temperature and the level of quantum fluctuations, along with inducing ferrimagnetic domains. Yet, perhaps one should not be too expedient in assuming a generic irrelevance of long-range dipolar interactions of order 10^{-1} compared to J_{zz} for any candidate quantum spin ice material. One can imagine that dipolar interactions may play an important role, possibly inducing novel phases, in a material that would, based solely on its effective anisotropic exchange couplings $\{J_e\}$, find itself at the boundary between the various semiclassical and intrinsically quantum phases identified in mean-field lattice gauge theories of quantum spin ices.[21,22]

It is useful at this point to discuss how our results fit with the current state of affairs regarding $Yb_2Ti_2O_7$. For the values $J_e = J_{zz}, J_{z\pm}, J_{\pm}, J_{\pm\pm}$ for model (1) that we used, mean-field theory[20] predicts a long-range-ordered ferromagnetic state with a nonsaturated magnetization along one of the $\langle 100 \rangle$ axes, and with the magnetic moment at each site splayed away from the magnetization direction. The same splayed-ferromagnetic (*sp*-FM) state phase is predicted on the basis of a gauge mean-field theory (g-MFT).[21] Indeed, on the basis of the latter work, $Yb_2Ti_2O_7$ would be predicted to be located deep in the *sp*-FM phase, far from the phase boundary with an antiferromagnetic state as well as far from a U(1) quantum spin liquid state or the exotic Coulomb ferromagnetic state. The results presented in this paper [see discussion of the field and temperature dependence of $C(T,h)$ and $S(T,h)$ in relation to Figs. 6 and 7] suggest that the model is developing correlations that would, below the lowest temperature where the current NLC calculations are reliable, lead to this *sp*-FM phase.

One notes that the *sp*-FM phase is the one that has been reported in a recent neutron scattering experiment on a single crystal,[40] as suggested by earlier studies.[37] However, other single-crystal neutron scattering experiments,[20,39] neutron depolarization measurements[38] and muon spin relaxation studies[41] have not confirmed such a *sp*-FM state. In the same vein, and rather interestingly, a very recent work on the closely related $Yb_2Sn_2O_7$ material[45] has found a sharp first-order

transition at $T_c \sim 0.15$ K to a state, which according to ^{170}Yb Mössbauer spectroscopy and powder neutron scattering, is precisely a *sp*-FM phase.[45]

If the *sp*-FM phase is a natural state for the $Yb_2M_2O_7$ (M = Ti, Sn) materials, why then does $Yb_2Ti_2O_7$ fail to display a robust *sp*-FM ordering? The answer to this question may be partly related to the recent evidence that there is a tendency for a small percentage [O(1%)] of Yb^{3+} to occupy Ti^{4+} sites in single crystals grown via the image furnace method.[44] This phenomenon is referred to as "stuffing." Such a form of disorder would lead to effective random bonds being generated between the original Yb^{3+} pyrochlore lattice ions. Naively, one might have thought that if such frustrating random bonds were sufficiently strong to fully undermine the development of the *sp*-FM phase, the system would then go into a spin glass state. However, to the best of our knowledge, no experiment has reported evidence for a spin glass state in $Yb_2Ti_2O_7$.[38,41,75] In light of the observation that single-crystal samples may be prone to stuffing and that some powder samples display very sharp specific-heat anomaly,[44] it might be worthwhile to carry out a new generation of powder neutron scattering measurements on samples with the sharpest specific-heat anomaly.[44]

In summary, our results confirm the values of the anisotropic exchange previously determined in Ref. 20. In the simplest scenario, these couplings would lead to a ferromagnetic phase with moments splayed away from the ⟨100⟩ axes. What prevents $Yb_2Ti_2O_7$ to enter this state is at this time not known. Until the nature of the state below $T_c \sim 0.26$ K has been determined experimentally and understood theoretically, the problem of $Yb_2Ti_2O_7$ will not have been completely solved.

Let us conclude with a few general comments. We believe that it would be, at this time, very interesting and most useful to carry out similar studies that combine inelastic neutron scattering and thermodynamic bulk measurements for other candidate quantum spin ice materials, with $Yb_2Sn_2O_7$ (Ref. 45) and $Yb_2Ge_2O_7$ being obvious choices. From the lessons learned in this work, as well as from Ref. 63, we anticipate that NLC will contribute to help developing a quantitative parametrization of microscopic models of quantum spin ices and help pave the way for an ultimate understanding of these fascinating systems. However, for this program to be successful, the availability of high-resolution inelastic neutron scattering data sets will likely prove to be essential. In parallel, in-field single-crystal specific-heat and magnetization measurements which properly account for demagnetization effects will also be necessary.

Note added in proof. Recently, a transition at a temperature 0.15 K to a canted ferromagnetic phase in $Yb_2Sn_2O_7$, a close analog of $Yb_2Ti_2O_7$, was reported.[45] On the other hand, another study on $Yb_2Sn_2O_7$ did not find evidence for such a long-range ordered canted ferromagnetic phase.[78]

ACKNOWLEDGMENTS

We acknowledge useful discussions with P. Dalmas de Réotier, B. Javanparast, P. McClarty, J. Quilliam, J. Thompson, and A. Yaouanc. This work is supported in part by NSF Grant No. DMR-1004231, the NSERC of Canada, the Canada Research Chair program (M.J.P.G., Tier 1) and by the Perimeter Institute for Theoretical Physics. Research at the Perimeter Institute is supported by the Government of Canada through Industry Canada and by the Province of Ontario through the Ministry of Economic Development & Innovation.

[1] L. Balents, Nature (London) **464**, 199 (2010).

[2] The pairwise interactions themselves could be ferromagnetic but be frustrated by strong local single-ion anisotropy with local axis that form an angle larger than 90°, as arises in spin ice compounds. In that case, the *effective* interactions can be said to be antiferromagnetic (see Ref. 3).

[3] M. J. P. Gingras, in *Introduction to Frustrated Magnetism*, Springer Series in Solid-State Sciences, Vol. 164, edited by C. Lacroix, P. Mendels, and F. Mila (Springer, Berlin, 2011), Chap. 12.

[4] R. Moessner, Can. J. Phys. **79**, 1283 (2001).

[5] J. S. Gardner, M. J. P. Gingras, and J. E. Greedan, Rev. Mod. Phys. **82**, 53 (2010).

[6] J. D. M. Champion, M. J. Harris, P. C. W. Holdsworth, A. S. Wills, G. Balakrishnan, S. T. Bramwell, E. Cižmár, T. Fennell, J. S. Gardner, J. Lago, D. F. McMorrow, M. Orendáč, A. Orendáčová, D. McK. Paul, R. I. Smith, M. T. F. Telling, and A. Wildes, Phys. Rev. B **68**, 020401 (2003).

[7] L. Savary, K. A. Ross, B. D. Gaulin, J. P. C. Ruff, and Leon Balents, Phys. Rev. Lett. **109**, 167201 (2012); M. E. Zhitomirsky, M. V. Gvozdikova, P. C. W. Holdsworth, and R. Moessner, *ibid.* **109**, 077204 (2012); J. Oitmaa, R. R. P. Singh, A. G. R. Day, B. V. Bagheri, and M. J. P. Gingras, arXiv:1305.2935 (2013).

[8] J. R. Stewart, G. Ehlers, A. S. Wills, S. T. Bramwell, and J. S. Gardner, J. Phys.: Condens. Matter **16**, L321 (2004).

[9] J. S. Gardner, S. R. Dunsiger, B. D. Gaulin, M. J. P. Gingras, J. E. Greedan, R. F. Kiefl, M. D. Lumsden, W. A. MacFarlane, N. P. Raju, J. E. Sonier, I. Swainson, and Z. Tun, Phys. Rev. Lett. **82**, 1012 (1999).

[10] M. J. Harris, S. T. Bramwell, P. C. W. Holdsworth, and J. D. M. Champion, Phys. Rev. Lett. **81**, 4496 (1998).

[11] S. T. Bramwell, M. J. Harris, B. C. den Hertog, M. J. P. Gingras, J. S. Gardner, D. F. McMorrow, A. R. Wildes, A. L. Cornelius, J. D. M. Champion, R. G. Melko, and T. Fennell, Phys. Rev. Lett. **87**, 047205 (2001).

[12] A. P. Ramirez, A. Hayashi, R. J. Cava, R. Siddharthan, and B. S. Shastry, Nature (London) **399**, 333 (1999).

[13] S. T. Bramwell and M. J. P. Gingras, Science **294**, 1495 (2001).

[14] C. Castelnovo, R. Moessner, and S. L. Sondhi, Annu. Rev. Condens. Matter Phys. **3**, 35 (2012).

[15] A. L. Cornelius and J. S. Gardner, Phys. Rev. B **64**, 060406 (2001).

[16] H. D. Zhou, J. G. Cheng, A. M. Hallas, C. R. Wiebe, G. Li, L. Balicas, J. S. Zhou, J. B. Goodenough, J. S. Gardner, and E. S. Choi, Phys. Rev. Lett. **108**, 207206 (2012).

[17] C. L. Henley, Annu. Rev. Condens. Matter Phys. **1**, 179 (2010).

[18]C. Castelnovo, R. Moessner, and S. L. Sondhi, Nature (London) **451**, 42 (2008).
[19]R. R. P. Singh, Physics **4**, 77 (2011).
[20]K. A. Ross, L. Savary, B. D. Gaulin, and L. Balents, Phys. Rev. X **1**, 021002 (2011).
[21]L. Savary and L. Balents, Phys. Rev. Lett. **108**, 037202 (2012).
[22]S. B. Lee, S. Onoda, and L. Balents, Phys. Rev. B **86**, 104412 (2012).
[23]The pyrochlore lattice can be described by a face-centered-cubic (fcc) space lattice with a four-site (tetrahedron) sublattice basis. The $\hat{z}$ quantization axis is along the local [111] cubic direction at each of the four sublattice sites, and $\pm$ (or equivalently, x and y) refers to the two orthogonal local directions.
[24]The "transverse" [to the local [111] direction (Ref. 23)] $\langle\psi^{\pm}|J^{\pm}|\psi^{\mp}\rangle$ matrix elements determine the Zeeman energy splitting for a hypothetical magnetic field applied perpendicular to the local [111] at a given site and which determines the g_{xy} component of the g tensor.
[25]M. J. P. Gingras and P. Henelius, J. Phys.: Conf. Series **320**, 012001 (2011).
[26]$Pr_2Ti_2O_7$ forms a monoclinic structure rather than a pyrochlore one. See Ref. 5.
[27]H. R. Molavian, M. J. P. Gingras, and B. Canals, Phys. Rev. Lett. **98**, 157204 (2007).
[28]H. R. Molavian, P. A. McClarty, and M. J. P. Gingras, arXiv:0912.2957.
[29]S. Onoda and Y. Tanaka, Phys. Rev. B **83**, 094411 (2011).
[30]S. Rosenkranz, A. P. Ramirez, A. Hayashi, R. J. Cava, R. Siddharthan, and B. S. Shastry, J. Appl. Phys. **87**, 5914 (2000).
[31]A. Bertin, Y. Chapuis, P. Dalmas de Réotier, and A. Yaouanc, J. Phys.: Condens. Matter **24**, 256003 (2012).
[32]B. C. den Hertog and M. J. P. Gingras, Phys. Rev. Lett. **84**, 3430 (2000).
[33]T. Yavorsk'ii, T. Fennell, M. J. P. Gingras, and S. T. Bramwell, Phys. Rev. Lett. **101**, 037204 (2008).
[34]B. Z. Malkin, T. T. A. Lummen, P. H. M. van Loosdrecht, G. Dhalenne, and A. R. Zakirov, J. Phys.: Condens. Matter **22**, 276003 (2010).
[35]J. A. Hodges, P. Bonville, A. Forget, A. Yaouanc, P. Dalmas de Réotier, G. André, M. Rams, K. Królas, C. Ritter, P. C. M. Gubbens, C. T. Kaiser, P. J. C. King, and C. Baines, Phys. Rev. Lett. **88**, 077204 (2002).
[36]H. W. J. Blöte, R. F. Wielinga, and W. J. Huiscamp, Physica (Amsterdam) **43**, 549 (1969).
[37]Y. Yasui, M. Soda, S. Iikubo, M. Ito, M. Sato, N. Hamaguchi, T. Matsushita, N. Wada, T. Takeuchi, N. Aso, and K. Kakurai, J. Phys. Soc. Jpn. **72**, 3014 (2003).
[38]J. S. Gardner, G. Ehlers, N. Rosov, R. W. Erwin, and C. Petrovic, Phys. Rev. B **70**, 180404 (2004).
[39]K. A. Ross, J. P. C. Ruff, C. P. Adams, J. S. Gardner, H. A. Dabkowska, Y. Qiu, J. R. D. Copley, and B. D. Gaulin, Phys. Rev. Lett. **103**, 227202 (2009).
[40]L.-J. Chang, S. Onoda, Y. Su, Y.-J. Kao, K.-D. Tsuei, Y. Yasui, K. Kakurai, and M. R. Lees, Nat. Commun. **3**, 992 (2012).
[41]R. M. D'Ortenzio, H. A. Dabkowska, S. R. Dunsiger, B. D. Gaulin, M. J. P. Gingras, T. Goko, J. B. Kycia, L. Liu, T. Medina, T. J. Munsie, D. Pomaranksi, K. A. Ross, Y. J. Uemura, T. J. Williams, and G. M. Luke, arXiv:1303.3850.
[42]A. Yaouanc, P. Dalmas de Réotier, C. Marin, and V. Glazkov, Phys. Rev. B **84**, 172408 (2011).
[43]K. A. Ross, L. R. Yaraskavitch, M. Laver, J. S. Gardner, J. A. Quilliam, S. Meng, J. B. Kycia, D. K. Singh, Th. Proffen, H. A. Dabkowska, and B. D. Gaulin, Phys. Rev. B **84**, 174442 (2011).
[44]K. A. Ross, Th. Proffen, H. A. Dabkowska, J. A. Quilliam, L. R. Yaraskavitch, J. B. Kycia, and B. D. Gaulin, Phys. Rev. B **86**, 174424 (2012).
[45]A. Yaouanc, P. Dalmas de Réotier, P. Bonville, J. A. Hodges, V. Glazkov, L. Keller, V. Sikolenko, M. Bartkowiak, A. Amato, C. Baines, P. J. C. King, P. C. M. Gubbens, and A. Forget, Phys. Rev. Lett. **110**, 127207 (2013).
[46]J. Lago, I. Zivkovic, B. Z. Malkin, J. Rodriguez Fernandez, P. Ghigna, P. Dalmas de Reotier, A. Yaouanc, and T. Rojo, Phys. Rev. Lett. **104**, 247203 (2010).
[47]J. Villain, Z. Phys. B: Condens. Matter Quanta **33**, 31 (1979).
[48]M. Hermele, M. P. A. Fisher, and L. Balents, Phys. Rev. B **69**, 064404 (2004).
[49]A. H. Castro-Neto, P. Pujol, and E. Fradkin, Phys. Rev. B **74**, 024302 (2006).
[50]A. Banerjee, S. V. Isakov, K. Damle, and Y.-B. Kim, Phys. Rev. Lett. **100**, 047208 (2008).
[51]N. Shannon, O. Sikora, F. Pollmann, K. Penc, and P. Fulde, Phys. Rev. Lett. **108**, 067204 (2012).
[52]P. Bonville, I. Mirebeau, A. Gukasov, S. Petit, and J. Robert, Phys. Rev. B **84**, 184409 (2011).
[53]S. Petit, P. Bonville, I. Mirebeau, H. Mutka, and Julien Robert, Phys. Rev. B **85**, 054428 (2012).
[54]O. Benton, O. Sikora, and N. Shannon, Phys. Rev. B **86**, 075154 (2012).
[55]Unlike $Tb_2(Ti, Sn)_2O_7$ (Refs. 27 and 28) the energy gap to the first excited crystal field state in $Pr_2(Sn, Zr)_2O_7$ and $Yb_2Ti_2O_7$ is large compared to the interactions $H_{\rm int}$. This allows one to consider a spin-$\frac{1}{2}$ effective low-energy theory that contains a one-to-one mapping of the $\langle|\psi^{\pm}|J_i^u|\psi^{\mp}|\rangle$ matrix elements (see discussion in Supplemental Material of Ref. 56) without concerns about interaction-induced admixing between the crystal-field levels (see Refs. 27 and 28).
[56]J. D. Thompson, P. A. McClarty, H. M. Rønnow, L. P. Regnault, A. Sorge, and M. J. P. Gingras, Phys. Rev. Lett. **106**, 187202 (2011).
[57]S. H. Curnoe, Phys. Rev. B **78**, 094418 (2008).
[58]P. A. McClarty, S. H. Curnoe, and M. J. P. Gingras, J. Phys.: Conf. Ser. **145**, 012032 (2009).
[59]M. J. P. Gingras and B. C. den Hertog, Can. J. Phys. **79**, 1339 (2001).
[60]S. V. Isakov, R. Moessner, and S. L. Sondhi, Phys. Rev. Lett. **95**, 217201 (2005).
[61]H. Cao, A. Gukasov, I. Mirebeau, P. Bonville, C. Decorse, and G. Dhalenne, Phys. Rev. Lett. **103**, 056402 (2009).
[62]H. B. Cao, A. Gukasov, I. Mirebeau, and P. Bonville, J. Phys.: Condens. Matter **21**, 492202 (2009).
[63]R. Applegate, N. R. Hayre, R. R. P. Singh, T. Lin, A. G. R. Day, and M. J. P. Gingras, Phys. Rev. Lett. **109**, 097205 (2012).
[64]M. Rigol, T. Bryant, and R. R. P. Singh, Phys. Rev. Lett. **97**, 187202 (2006); Phys. Rev. E **75**, 061118 (2007); **75**, 061119 (2007).
[65]R. R. P. Singh and J. Oitmaa, Phys. Rev. B **85**, 144414 (2012).
[66]See, for example, W. H. Press *et al.*, *Numerical Recipes* (Cambridge University Press, Cambridge, UK, 1989), p. 133.
[67]J. S. Gardner, B. D. Gaulin, and D. McK. Paul, J. Cryst. Growth **191**, 740 (1998).
[68]A. Aharoni, J. Appl. Phys. **83**, 3432 (1998).
[69]J. D. Thompson, P. A. McClarty, and M. J. P. Gingras, J. Phys.: Condens. Matter **23**, 164219 (2011).

[70]J. D. Thompson, M.S. thesis, University of Waterloo, 2011. Some comments in this document as per the merit of using RPA to fit the diffuse neutron scattering of $Yb_2Ti_2O_7$ at $T_{fit} = 1.4$ K as opposed to the other data set at 9.1 K are of relevance to the present discussion. Citing an extract from p. 49: "We choose to use the data collected at $T = 1.4$ K rather than the data collected at $T = 9.1$ K as the signal to noise ratio of this data is higher. In principal [sic] the $T = 9.1$ K data would have better suited our purpose, as at this temperature $Yb_2Ti_2O_7$ is situated much more firmly in the paramagnetic phase, avoiding any potential problems with $Yb_2Ti_2O_7$ being in a collective paramagnetic phase, and correlation effects that appear due to the presence of a nearby phase transition."

[71]The quantitative failure of a quantum spin ice Hamiltonian $\mathcal{H}_{QSI}$ with anisotropic exchange couplings obtained from a random phase approximation (RPA) fit of the diffused neutron scattering, as reported in both Refs. 40 and 56, to describe the zero-field magnetic specific heat had already been pointed out in Ref. 63.

[72]J. P. C. Ruff, J. P. Clancy, A. Bourque, M. A. White, M. Ramazanoglu, J. S. Gardner, Y. Qiu, J. R. D. Copley, M. B. Johnson, H. A. Dabkowska, and B. D. Gaulin, Phys. Rev. Lett. **101**, 147205 (2008).

[73]P. Dalmas de Réotier, A. Yaouanc, Y. Chapuis, S. H. Curnoe, B. Grenier, E. Ressouche, C. Marin, J. Lago, C. Baines, and S. R. Giblin, Phys. Rev. B **86**, 104424 (2012).

[74]We note, however, that no magnetic Bragg peaks were found in the neutron diffraction pattern of the powder sample studied in Ref. 35, but which nevertheless display a fairly sharp specific-heat feature at $T_c \sim 0.24$ K [see Fig. 4 in P. Dalmas de Réotier, V. Glazkov, C. Marin, A. Yaouanc, P. C. M. Gubbens, S. Sakarya, P. Bonville, A. Amato, C. Baines, and P. J. C. King, Physica B (Amsterdam) **374–375**, 145 (2005)], albeit not as sharp as that found in another powder sample studied in Ref. 44.

[75]In fact, muon spin relaxation (μSR) on $Yb_2Ti_2O_7$ does not find a static moment below $T_c \sim 0.26$ K (Refs. 35 and 41). Perhaps it must be said that μSR results in the $R_2M_2O_7$ have proven perplexing (Refs. 76 and 77). For example, while Mössbauer and neutron scattering find an ordered state in $Yb_2Sn_2O_7$ (Ref. 45) μSR finds that the magnetic moment continue to fluctuate down to the lowest temperature considered.

[76]P. A. McClarty, J. N. Cosman, A. G. Del Maestro, and M. J. P. Gingras, J. Phys.: Condens. Matter **23**, 164216 (2011).

[77]P. Quémerais, P. A. McClarty, and R. Moessner, Phys. Rev. Lett. **109**, 127601 (2012).

[78]Z. L. Dun, E. S. Choi, H. D. Zhou, A. M. Hallas, H. J. Silverstein, Y. Qiu, J. R. D. Copley, J. S. Gardner, and C. R. Wiebe, Phys. Rev. B **87**, 134408 (2013).